Bulgarian Chemical Communications, Volume 51, Issue 3, pp. (433 – 438) 2019 DOI: 10.34049/bcc.51.3.5111

Mechanochemically synthesized N-doped ZnO for photodegradation of ciprofloxacin

N.G. Kostova[1*], M. Fabian[2], E. Dutkova[2]

[1] *Institute of Catalysis, Bulgarian Academy of Sciences, Acad. G. Bonchev St., Bldg. 11, 1113 Sofia, Bulgaria*
[2] *Institute of Geotechnics, Slovak Academy of Science, 04001 Kosice, Slovakia*

Received: February 5, 2019; Revised: June 14, 2019

N-doped ZnO photocatalyst was prepared using mechanochemical method with ammonium hydroxide as nitrogen source (ZnO-am). The mechanical activated ZnO sample was also prepared for comparison (ZnO-MA). As-milled samples were calcined at 673 K. The so prepared samples have been characterized by X-ray diffraction (XRD), diffuse reflectance (DRS) and photoluminescence (PL) spectroscopy The XRD analysis shows wurtzite crystal structure of synthesized samples. The positions of diffraction peaks of mechanochemically synthesized nanostructured sample were shifted to slightly higher angles. The crystallite size decreased from 168 to 35 nm. Only a strong absorption band was registered in the UV region in the DRS spectrum of initial ZnO, while in the spectrum of N-doped ZnO-am sample absorption in the visible light region was also observed. All the samples were tested as photocatalytic materials in the model reaction of ciprofloxacin (CIP) photodegradation. The lower PL intensity of ZnO-am indicates a lower recombination rate of photoexcited electrons and holes. Doping nitrogen a new electron energy level is created inside the band gap of ZnO. The ZnO-am nanostructured sample has higher photocatalytic activity under visible light irradiation.

Keywords: mechanochemistry, ZnO, doping, photoluminescence, photocatalysis, visible light

INTRODUCTION

During the past several decades aqueous organic contaminants such as antibiotics discharged from industrial activities and hospitals have become increasingly harmful to human health and environment. Ciprofloxacin (CIP), a broad spectrum second generation fluoroquinolone class of antibiotic drug, has been widely used to fight against variety diseases [1]. CIP exists in different water resources such as wastewater, surface water or ground water. The drug could not be easily biodegraded during biological wastewater treatment process. Recently, the removal of environmental pollutants based on solar energy-driven semiconductor photocatalysis has been developed [2]. Zinc oxide, known as multifunctional materials, was subject of extensive studies as a photocatalysts due to its low price, non-toxicity and wide band gap [3]. Disadvantage of ZnO is its low photocatalytic activity under illumination with visible light. Diminishing the band gap of ZnO by non-metal doping is considered as one of the most effective strategies to improve the photocatalytic activity. Nitrogen is the best choice as it has nontoxicity, lower electronegativity and ionization energy than the oxygen atom. Various methods have been applied for doping nitrogen to ZnO – e.g. precipitation [4], microwave irradiation [5], sol-gel [6], thermal decomposition [7], microwave-assisted hydrothermal method [8], microemulsion method [9], combustion method [10] and mechanochemical synthesis [11]. The latter method enables obtaining considerable quantities of materials in an economic way [12]. During the last years the mechanochemistry is being applied successfully for the preparation of catalysts [13], sulphides [14], perovskites [15], mixed oxides [16], as well as for doping oxides with metals and non-metals [17]. The mechanical grinding or milling often leads to the formation of defects in the materials. Their transformation into stable phases was induced by means of additional calcination, which cannot be achieved by most of the conventional methods [18]. In contrast to the most often applied sol-gel method for the synthesis of nitrogen-doped zinc oxide photocatalysts, the mechanochemical synthesis is an environment friendly method, which does not use toxic organic solvents [19].

In the present paper we provide a detailed analysis of the majority of properties of mechano-chemically treated ZnO-am and a proof of its photocatalytic activity in photodegradation of pollu-tants in waste water under visible light irradiation.

* To whom all correspondence should be sent
E-mail: nkostova@ic.bas.bg

EXPERIMENTAL

Materials

ZnO (Chimsnab Bulgaria AD), ammonia solution (NH_4OH, 28%, density 0.918 g/mL) (Neochim AD, Bulgaria) and ciprofloxacin (Sigma Aldrich, Germany) were used without further purification.

Preparation and characterization of N-doped photocatalyst

N-doped ZnO sample was prepared by mechanochemical synthesis from ZnO, and ammonia solution using a high-energy planetary ball mill Pulverisette 6 (Fritsch, Germany). The precursors were milled for 30 min at 550 rpm in ambient atmosphere using a chamber of 250 cm^3 with 21 balls of 10 mm in diameter all made of zirconia. The ball-to-powder mass ratio was 40:1. After milling, the powdered mixture was calcined 2 h at 673 K. The sample was referred to as ZnO-am. The sample prepared by ball milling of zinc oxide without nitrogen source was named ZnO-MA.

The X-ray diffraction (XRD) patterns were recorded on a D8 Advance diffractometer (Brucker, Germany) using CuK_α radiation. The diffraction data were collected in the range of $20° < 2\Theta < 65°$, with steps of 0.02° and a counting time of 9 s/step. The crystallite sizes were calculated applying Scherrer's equation.

UV–Vis spectra for evaluation of photophysical properties were recorded in diffuse reflectance mode (DRS) and transformed into absorption spectra through the Kubelka-Munk function [20]. A Thermo Evolution 300 UV-Vis Spectrophotometer, equipped with a Praying Mantis device with Spectralon as the reference was used.

The photoluminescence (PL) spectra at room temperature were acquired on a photon counting spectrofluorometer PC1 (ISS) with a photoexcitation wavelength of 325 nm. A 300 W xenon lamp was used as the excitation source. For measuring the PL intensity, the powders were suspended in absolute ethanol.

Photocatalytic procedure

Photodegradation of ciprofloxacin was carried out in a semi-batch slurry reactor containing 0.1 g catalyst and 100 mL of 10 $mg \cdot L^{-1}$ CIP solution at 298 K under visible light. Prior to illumination, the suspensions were continuously stirred in dark for 30 min to ensure the adsorption/desorption equilibrium of the CIP on the photocatalyst powders. The suspension was then irradiated by visible light LED lamp (10 W) with distance 7 cm from the surface of the slurry. At regular time interval, aliquot samples were taken and centrifuged to eliminate the photocatalyst. The concentration of CIP during the photocatalytic reaction was estimated using Spekol 11 (Carl Zeiss, Germany) spectrophotometer at 277 nm at room temperature. Each sample was turned back to the reaction mixture after the spectrophotometric measurement. All photocatalytic tests were performed at constant stirring rate of 400 rpm in presence of air flow and at room temperature.

RESULTS AND DISCUSSION

X-ray diffraction (XRD) was used to identify the crystalline phase structure of the samples. Fig. 1 represents the diffraction patterns of the initial ZnO and mechanochemically synthesized samples. The diffraction pattern of the initial ZnO displays sharp intensive peaks, identified as due to (100), (002), (101), (102) and (110) planes. The observed diffracttion lines in the patterns of the mechanochemically treated samples are in accordance with those of hexagonal ZnO having wurtzite structure (JCPDS card 89-7102). No peaks of other phases have been registered.

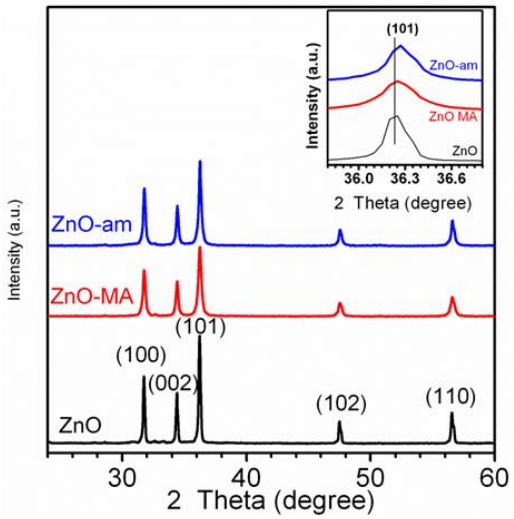

Fig. 1. XRD patterns of initial ZnO, ZnO-MA and ZnO-am samples.

After 30 minutes of mechanical treatment small differences were registered in the relative intensities of the diffraction lines. The decrease in intensity of the diffraction lines is larger in the diffraction pattern of ZnO-MA, while that of the nitrogen doped sample is not so distinctly expressed. The crystallites size was calculated based on the full width at half maximum (FWHM) of the peak (101) applying the equation of Scherrer. The average crystallites sizes are listed in Table 1.

Table 1. Lattice parameters, crystallites size and energy band gap of ZnO, ZnO-MA and ZnO-am samples

Sample	Lattice parameter (Å)		Crystallites size	Energy band gap	rate constant *k*
	a = b	c	(nm)	(eV)	(min^{-1})
ZnO	3.251(6)	5.209(4)	168	3.19	0.0007
ZnO-MA	3.252(1)	5.210(2)	32	2.54	0.0035
ZnO-am	3.249(2)	5.205(3)	35	1.74	0.0062

The lattice parameters of ZnO-MA sample increased after mechanical treatment which is consistent with the literature [21]. Nitrogen doping of ZnO led to reduction of the lattice parameters of ZnO-am sample (Table 1).The registered widening of the diffraction peaks in the XRD patterns of the mechanochemically synthesized samples witnesses decrease in the crystallites size from 168 nm for the initial ZnO down to 32 (35) nm for the other samples. A slight shift of the diffraction peaks to larger angle positions was observed in the dif-fraction patterns of the mechanochemically treated samples in comparison with the pure ZnO (inset of Fig. 1). On the other hand, our results differ from those of Dai *et all*. [22], where diffraction peak shifts toward lower angles was reported. The shift to the larger angle positions is within 0.015° for the sample ZnO-MA and 0.03° for the sample ZnO-am and, that is evidence for the formation of oxygen defects. The registered changes in the diffraction patterns could be explained with local modification of the structure occurring during the ball milling and stabilized in the consecutive thermal treatment [23].

The optical properties of the samples were investigated by means of PL and DRS. PL spectra supply information about the recombination of the photogenerated charges [24]. The photolumi-nescence spectra of the initial ZnO and those of the mechanochemically synthesized samples, dispersed in ethanol, are represented in Fig. 2.

The PL spectra of all samples contain a high intensity peak at 384 nm and low intensive bands at about 425, 467 and 530 nm. The strong UV emis-sion can be assigned to a near-band-edge (NBE) emission originating from recombination of excited electrons in a localized level below the conduction band with holes in the valence band. In addition a slight shift of the UV peak is registered towards higher wavelength region in the PL spectra of ZnO-am and mechanically activated ZnO sample.

The registered significant widening of the band gives evidence for super-positioning of violet emission upon the UV emission, which can be assigned to electrons from the shallow neutral donor level to the upper level of the valence band [25-26]. The sharp decrease in intensity of the bands in the photoluminescence spectra of the mechanochemically synthesized samples indicates a lower recombination rate of electron-hole pairs. It has been generally accepted that the highly intensive photoluminescence means high degree of recombination of the photogenerated charge carriers (e^- and h^+), implying low photocatalytic activity [27] and vice versa - the low intensity of the emission bands in the photoluminescence spectrum means lower rate of recombination, which is assumption for high photocatalytic activity.

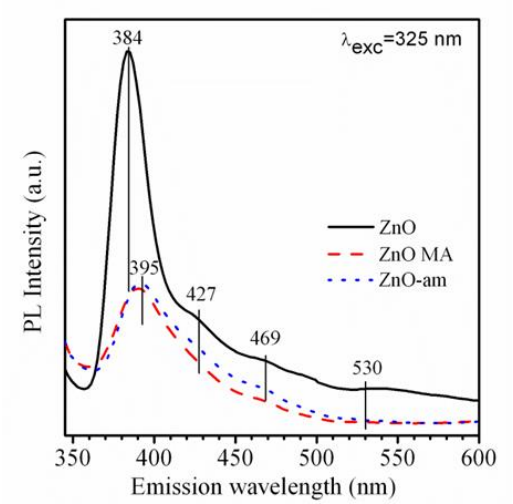

Fig. 2. Photoluminescence spectra of the initial ZnO, ZnO-MA and ZnO-am samples

UV-Vis diffuse reflectance spectra of the initial ZnO, the mechanically activated zinc oxide, as well as the mechanochemically treated samples, doped with nitrogen are shown in Fig. 3. In the ultraviolet region (200–360 nm) all the samples showed similar in intensity reflections. The optical spectrum of the initial sample is dominated by transition from the valence band to the conduction band, occurring at about 400 nm. Within the visible range of the spectra one can observe substantial differences in the spectra of the initial zinc oxide and the mechanochemically synthesized samples (Fig. 3). It is observable in the spectra of the mechano-chemically synthesized samples less intensive reflectance (more intensive absorbance) in the visible region from 400 up to 700 nm. In the reflectance spectra of ZnO-am sample was registered red shifting towards larger wavelengths in comparison with the initial ZnO. The more intensive absorbance in the visible region in the spectra of the

nitrogen-doped TiO_2 and ZnO is usually attributed to formation of oxygen vacancies, whereupon an additional electron energy level appears inside the band gap. Similar results have also been obtained by some other authors [28-29].

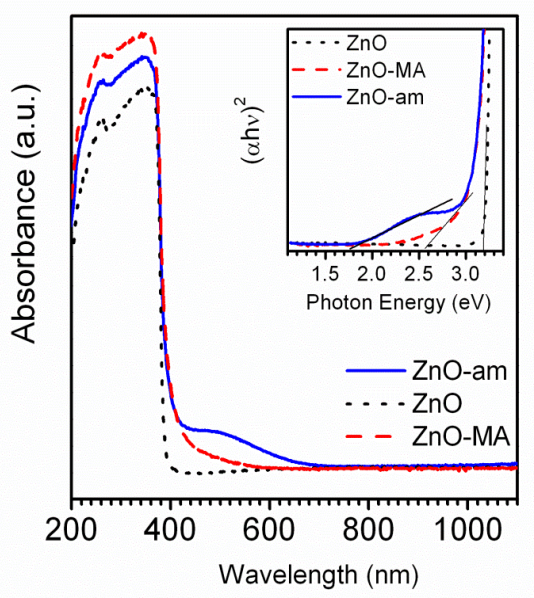

Fig. 3. Diffuse reflectance spectra (inset Tauc's plots) of the initial ZnO, ZnO-MA and ZnO-am samples.

The Tauc's method was applied for determining the band gap energy of the samples. The band gap of oxide semiconductors can be determined on the basis of the equation: $\alpha hv = A(hv - E_g)n$, where α is absorption coefficient, hv is the incident photon energy, A is a constant, n value is ½ for direct semiconductor [30]. The calculated values of the band gap energy are represented in Table 1. The band gap value obtained for the pristine ZnO sample (3.19 eV) is similar to other samples, synthesized by different methods [31]. After the doping the value of the band gap width is decreased down to 1.74 eV. It is obvious that the light-absorption edges of the mechanochemically treated samples exhibit a red-shift towards the visible region with respect to that of the initial ZnO sample. The initial ZnO sample is colored in white, while the mechanochemically synthesized samples doped with nitrogen are yellow, which is in accordance with their narrow band gap. This change in their color is connected with the presence of a second absorption band and it is the evidence for the creation of mid-gap state, located on the N 2p orbitals [32]. Nakamura et al. [33] supposed that the nitrogen doping is accompa-nied by a growing number of generated oxygen vacancies. As a result of this narrowing of the band gap of the doped titanium dioxide is manifested by shifting of the edge of the valence band due to mixing of N 2p and O 2p electron states and shifting of the lower edge of conduction band in positive direction due to oxygen vacancies (see the scheme in Fig. 5).

The photocatalytic activity of all samples was tested in oxidative degradation of the ciprofloxacin. The CIP concentration after irradiation for a definite time was measured by UV-Vis spectrophotometer at λ_{max} = 277 nm. Negligible change in CIP concentration was registered in absence of photocatalyst, indicating CIP itself is stable and barely degraded under visible illumination (Fig. 4). The initial ZnO showed very low activity in the photodegradation of the dye, which is due to its low absorbance of visible light (proved by DRS in Fig. 3). ZnO-am nanostructured sample manifested the highest photocatalytic activity under irradiation with visible light among all studied photocatalysts. The value of CIP degradation efficiency over ZnO, ZnO-MA and ZnO-am was calculated at 4.25, 19, and 31% respectively.

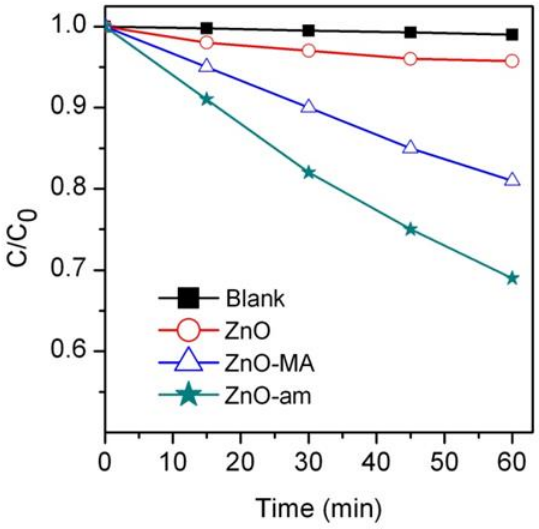

Fig. 4. Photodegradation of ciprofloxacin as a function of irradiation time of blank experiment without photocatalyst (■), initial ZnO (○), ZnO-MA (Δ) and ZnO-am (∗) under visible light irradiation.

Pseudo-first-order kinetics of photodegradation was supposed from the linear plot of $-\ln(C_0/C)$ versus irradiation time t and the rate constants are listed in Table 1. The results show that ZnO-am sample has the highest apparent rate constant indi-cating an obvious enhancement of catalytic activity for the mechanochemically synthesized sample.

There are several reasons for the observed higher photocatalytic activity of the nitrogen doped mechanochemically synthesized sample. The smaller size of the crystallites is important factor, which leads to enhance mobility of the charge to the surface and assistance in efficient participation in the photocatalytic process. The initial ZnO showed 5 x larger size of the crystallites (see Table 1) and very low

photocatalytic activity. Other factors exerting influence on the photocatalytic activity are the composition and the electronic structure of the samples. Nitrogen doping of the zinc oxide results in a new internal electron level formed by N 2p electrons inside the band gap of the semiconductor. CIP degradation is very complex. The scheme of possible reaction mechanism of photocatalytic degradation of CIP with of ZnO-am is represented in Fig. 5.

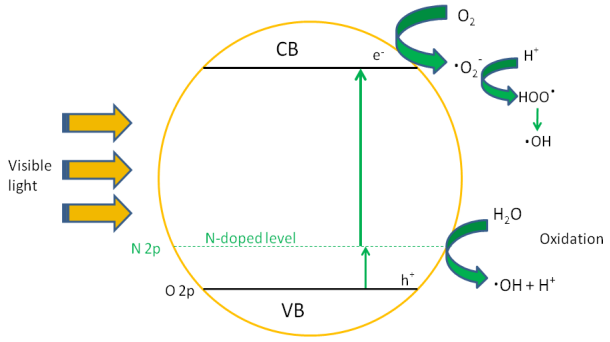

Fig. 5. Scheme of the possible reaction mechanism for the photocatalytic degradation of ciprofloxacin by ZnO-am under visible light irradiation.

The electrons removed from the valence band (VB) of ZnO upon irradiating with visible light are firstly excited to the newly formed electron energy level by visible light photons. Further, absorbing new photons they are transferred to the conduction band (CB) of ZnO. This means that the transfer of electron from VB to the CB in the ZnO-am sample can be realized through a two-stage transition even under irradiation by the lower energy visible light photons passing through the intermediate level N 2p. During the photocatalytic process the photo-generated electrons within the conduction band are migrating towards the surface and upon reacting with the oxygen molecules, adsorbed on the surface they form $\bullet O_2^-$ super oxide anion-radicals (Fig. 5). Further, they undergoes protonation forming HOO• hydroperoxide radicals. Mean-while the positively charged holes in the valence band migrate towards the surface and react with adsorbed H_2O molecules yielding the highly reactive hydroxyl radicals •OH. Both types of active particles (HOO• and •OH) initiate radical chain reaction mechanism leading to degradation of ciprofloxacin.

CONCLUSIONS

Nitrogen doped-ZnO nanostructured photocatalyst has been synthesized by the mechanochemical method applying ammonium hydroxide as nitrogen supplying precursor. Using photoluminescence spectroscopy it was found out that in the mechanochemically synthesized N-doped ZnO-am nanostructured sample the rate of recombination of the charge carriers is considerably lower. DRS results revealed that the absorption edge of the mechanochemically synthesized ZnO-am photocatalyst presents red shift compared to ZnO indicating an enhanced visible light absorption, which enables the utilization of these materials as photocatalysts for the purification of wastewaters operating under visible light irradiation.

Acknowledgements: The authors are grateful to the Bulgarian Science Fund for financial support by project DNTS/Slovakia 01/2.

REFERENCES

1. C. Bojer, J. Schbel, T. Martin, M. Ertl, H. Schmalz, Appl. Catal, B: Environ., 204, 561 (2017).
2. N. Kaneva, A. Bojinova, K. Papazova, D. Dimitrov, Bulg. Chem. Commun., **50**, Special issue H, 116 (2018).
3. A. di Mauro, M. E. Frgala, V. Privitera, G. Impellizzeri, Mater. Sci. Semicond. Processing, **69**, 44 (2017).
4. R. Kumari, A. Sahai, N. Goswami, Progress in Natural Science: Materials International, **25**, 300 (2015).
5. N. P. Herring,L. S. Panchakarla, M. Samy el-Shall, Langmuir, **30**, 2230 (2014).
6. J. J. Macias-Sanchez, L. Hinojosa-Reyes, A. Caballero-Quintero, W. de la Cruz , E. Ruiz-Ruiz, J. L. Hernandez-Ramirez, A. Guzman-Mar, Photochim. Photobiol. Sci., **14**, 536 (2015).
7. H. Sudrajat, S. Babel, Environ. Sci. Pollution Res., **23**, 10177 (2016).
8. G. Byzinski, C. Melo, D.P. Volanti, M. M. Ferrer, A. F. Gouveia, C. Ribeiro C, J. Andres, E. Longo, Mateials & Design, **120**, 363 (2017).
9. A. B. Lavang, Y. S. Malghe, J. Asian Ceram. Soc., **3**, 305 (2015).
10. G. Kale, S. Arbuj, U. Kawade, S. Rane, J. Ambekar, B. Kale, Materials Chemistry Frontiers, **2**, 163 (2018).
11. D. Chen, Z. Wang, T. Re, H. Ding, J. Phys. Chem. C, **118**, 15300 (2014).
12. A. F. Fuentes, L. Takacs, J. Mater. Sci., **48**, 598 (2013).
13. K. Ralphs, C. Hardacre, S. L. James, L. Stuart, Chem. Soc. Rev., **42**, 7701 (2013).
14. P. Balaz, M. Balaz, M. Achimovicova, Z. Bujnakova, E. Dutkova, J. Mater. Sci., 52, 11851 (2017).
15. Q. Zhang, F. Saito, Adv. Powder Technol., **23**, 523 (2012).
16. M. Senna, P. Billik, A. Y. Yermakov, M. Skratek. M. Majerova, J. Alloys Comp., **695**, 2314 (2017).
17. S. Livraghi, M. R. Chierotti, E. Giamello, G. Magnacca, M. C. Paganini, G. Cappelletti, C. L. Bianch, J. Phys. Chem. C, **112**, 17244 (2008).
18. M. L. Sanjuan, C. Guglieri, S. Diaz-Moreno, G.

Aquilanti, A. F. Fuentes, L. Olivi, J. Chaboy, Phys. Rev. B, **84**, 104207 (2011).
19. M. Balaz, A. Zorkovska, F. Urakaev, P. Balaz, J. Briancin, Z. Bujnakova, M. Achmovicova, E. Gock, RSC Adv., **6**, 87836 (2016).
20. T. B. Ivetic, M. R. Dimitrievska, N. L. Fincur, L. R. Dacanin, I. O. Guth, B. F. Abramovic, S. R. Lukic-Petrovic, Ceram. Inter., **40**, 1545 (2014).
21. J. Wang, Y. Xia, Y. Dong, R. Chen, L. Xiang, S. Komarneni, Appl. Catal. B: Environ., **192**, 8 (2016).
22. J. Dai, M-H. Yuan, J-H. Zeng, Q-F. Dai, S. Lan, C. Xiao, S-L. Tie, Optical Express, **23**, 29231 (2015).
23. Z. Petrovic, M. Ristic, S. Music, M. Fabian, Croat. Chem. Acta, **90**,135 (2017).
24. S. K. Mishra, R. K. Srivastava, S. G. Prakash, R. S. Yadav, A. C. Pandey, Optoeletron Rev., **18**, 467 (2010).
25. A. B. Lavand, Y. S. Malghe, J. King Saud University – Science, **30**, 65 (2018).
26. X. Feng, H. Guo, K. Patel, H. Zhou, X. Lou, Chem. Eng. J., **244**, 3227 (2014).
27. N. D. Abrazovic, M. Montone, L. Mirenghi, I. A. Jankovic, M. I. Comor, J. Nanosci. Nanotechnol., **8**, 613 (2008).
28. W. R. Lambrecht, A. Boonchum, Phys. Rev. B, **87**, 195 (2013).
29. M. Mapa, C. S. Gopinath, Chem. Mater., **21**, 351 (2009).
30. D. Chen, L. Gao, A. Yasumori, K. Kuroda, Y. Sugahara, Small, **4**, 1813 (2008).
31. B. Chavillon, L. Cario, A. Renaud, F. J. Amer. Chem. Soc., **134**, 464 (2012).
32. O. Game, U. Singh, A. A. Gupta, A. Suryawanshi, A. Anpurkar, S. Ogale, J. Mater. Chem., **22**, 17302 (2012)
33. R. Nakamura, T. Tanaka, Y. Nakato, J. Phys. Chem. B, **108**, 10617 (2004).